Global Ecology and Biogeography, (Global Ecol. Biogeogr.) (2006) **15**, 567–577

RESEARCH PAPER

Implementing plant hydraulic architecture within the LPJ Dynamic Global Vegetation Model

Thomas Hickler[1]*, I. Colin Prentice[2], Benjamin Smith[1], Martin T. Sykes[1] and Sönke Zaehle[3]†

[1]*Department of Physical Geography and Ecosystems Analysis, Geobiosphere Science Centre, Lund University, Sölvegatan 12, S-223 62 Lund, Sweden,* [2]*Department of Earth Sciences, University of Bristol, Wills Memorial Building, Queen's Road, Clifton, Bristol BS8 1RJ, UK, and* [3]*Potsdam Institute for Climate Impact Research, Global Change and Natural Resources Department, Telegrafenberg C4, D-14412 Potsdam, PO Box 601203, Germany*
†Present address: Laboratoire des Sciences du Climat et de l'Environment (LSCE), Orme des Merisiers, Bat. 712, F-91191 Gif-sur-Yvette Cedex, France.

*Correspondence: Thomas Hickler, Department of Physical Geography and Ecosystems Analysis, Geobiosphere Science Centre, Lund University, Sölvegatan 12, S-223 62 Lund, Sweden
E-mail: thomas.hickler@nateko.lu.se

ABSTRACT

Aim To implement plant hydraulic architecture within the Lund–Potsdam–Jena Dynamic Global Vegetation Model (LPJ–DGVM), and to test the model against a set of observational data. If the model can reproduce major patterns in vegetation and ecosystem processes, we consider this to be an important linkage between plant physiology and larger-scale ecosystem dynamics.

Location The location is global, geographically distributed.

Methods A literature review was carried out to derive model formulations and parameter values for representing the hydraulic characteristics of major global plant functional types (PFTs) in a DGVM. After implementing the corresponding formulations within the LPJ–DGVM, present-day model output was compared to observational data.

Results The model reproduced observed broad-scale patterns in potential natural vegetation, but it failed to distinguish accurately between different types of grassland and savanna vegetation, possibly related to inadequate model representations of water fluxes in the soil and wildfire effects. Compared to a version of the model using an empirical formulation for calculating plant water supply without considering plant hydraulic architecture, the new formulation improved simulated patterns of vegetation in particular for dry shrublands. Global-scale simulation results for runoff and actual evapotranspiration (AET) corresponded well to available data. The model also successfully reproduced the magnitude and seasonal cycle of AET for most EUROFLUX forests, while modelled variation in NPP across a large number of sites spanning several biomes showed a strong correlation with estimates from field measurements.

Main conclusions The model was generally confirmed by comparison to observational data. The novel model representation of water flow within plants makes it possible to resolve mechanistically the effects of hydraulic differences between plant functional groups on vegetation structure, water cycling, and competition. This may be an advantage when predicting ecosystem responses to nonextant climates, in particular in areas dominated by dry shrubland vegetation.

Keywords
Biomes, carbon cycle, evapotranspiration, global vegetation distribution, LPJ Dynamic Global Vegetation Model, NPP, plant hydraulic architecture, terrestrial ecosystem water balance.

INTRODUCTION

Terrestrial ecosystems provide fundamental services to society (e.g. Costanza *et al.*, 1997), and they interact through biophysical processes and biochemical exchanges with the atmosphere and the ocean (e.g. Foley *et al.*, 1994; Prentice *et al.*, 2001). Understanding the dynamics and functioning of terrestrial ecosystems is therefore an important challenge for environmental science, and necessary for predicting the likely future of the whole Earth system. In this context, different types of large-scale

© 2006 The Authors
Journal compilation © 2006 Blackwell Publishing Ltd
DOI: 10.1111/j.1466-822x.2006.00254.x
www.blackwellpublishing.com/geb

integrated biosphere models have become an important research tool.

Terrestrial biogeochemistry models have been widely applied to assess the potential effects of rising atmospheric CO_2 and climate change on terrestrial carbon storage and productivity (e.g. Melillo *et al.*, 1993; Schimel *et al.*, 2000). These models do not, however, account for changes in the distribution of vegetation types in response to climate change, which have been projected with equilibrium biogeography models (Prentice *et al.*, 1992; Neilson, 1995; Haxeltine & Prentice, 1996), in some cases as input into biogeochemistry models (VEMAP Members, 1995). Recently, both model types have been combined within dynamic global vegetation models (DGVMs), which simulate transient responses of ecosystem processes and distributions (e.g. Woodward *et al.*, 1995; Foley *et al.*, 1996; Friend & White, 2000; Kucharik *et al.*, 2000; Cramer *et al.*, 2001; Sitch *et al.*, 2003). This step required the explicit consideration of vegetation dynamic processes, and it mechanistically linked physiological processes on the level of plant organs, growth of individual trees, population dynamics, vegetation structure and ecosystem functioning on large scales. This is an advantage, because environmental effects on ecosystems are often driven by physiological processes on low levels of organization and small scales, such as photosynthetic assimilation in plant leaves (Mäkelä, 2003), and most detailed quantitative knowledge of biological responses to the environment concerns small-scale direct responses to environmental drivers (Luan *et al.*, 1996; Moorcroft *et al.*, 2001). DGVMs can be used to upscale this understanding to larger scales, at which many current ecological questions are posed (e.g. Houghton *et al.*, 2001). Furthermore, mechanistic model representations of physiological processes are more likely to hold true under changing environmental conditions, such as climate change, than empirically derived relationships concerning higher-level behaviour of the whole ecosystem.

In this study, we implemented a new formulation for modelling water flow between soils and leaves, which was based upon plant hydraulic architecture, within the Lund–Potsdam–Jena Dynamic Global Vegetation Model (LPJ–DGVM; Smith *et al.*, 2001; Sitch *et al.*, 2003). Plant hydraulic architecture refers to plant traits that influence the total resistance to water flow within plants, such as path lengths and conductivity of water-conducting tissues (roots, xylem and leaves; Zimmermann, 1978). Hydraulic plant characteristics in trees have been shown to influence the water supply to leaves and canopy conductance (Bond & Kavanagh, 1999; Schäfer *et al.*, 2000). Through the coupling of stomatal function and photosynthesis (Farquhar *et al.*, 1980), tree hydraulic architecture also constrains forest growth (Mencuccini & Grace, 1996; Ryan & Yoder, 1997; Tyree, 2003). Furthermore, strategic trade-offs that emerge from hydraulic constraints can determine the competitive balance between plants with different hydraulic characteristics (Sperry *et al.*, 2002). The effects of hydraulic architecture can become apparent directly, for example through decreasing water supply to the leaves as trees grow taller (Ryan & Yoder, 1997), or indirectly by plants allocating a variable proportion of assimilated carbon to non-photosynthetic tissue in order to minimize the effects of height on the water supply to leaves (Whitehead, 1998; Magnani *et al.*, 2000; McDowell *et al.*, 2002).

We carried out a literature review to derive model formulations and parameter values for representing the hydraulic characteristics of major global plant functional types (PFTs). Corresponding process formulations were implemented within LPJ–DGVM, and the model output was compared to observational data on global vegetation distribution, net primary productivity (NPP) and terrestrial ecosystem water balance. The data sets for model evaluation were chosen in order to represent vegetation and ecosystem processes that are likely to be sensitive to changes in the model formulations for calculating water availability and uptake through plants.

MATERIALS AND METHODS

The Lund–Potsdam–Jena Dynamic Global Vegetation Model (LPJ–DGVM)

The LPJ–DGVM is a coupled biogeography–biogeochemistry model which incorporates process-based representations of terrestrial vegetation dynamics and biogeochemical cycling (Smith *et al.*, 2001; Sitch *et al.*, 2003). The model has been widely applied to predict dynamic changes in ecosystem processes and is under ongoing development as a community model. It is a flexible framework for modelling terrestrial ecosystem structure and functioning. The LPJ–DGVM has also been incorporated into fully coupled earth system models, which have been used to analyse land cover feedbacks on the global carbon cycle (Joos *et al.*, 2001; Sitch *et al.*, 2005). The model has previously been shown, for example, to successfully reproduce the interannual global exchange of CO_2 with the atmosphere (Sitch *et al.*, 2003) and the observed high-latitude vegetation greening trend in the 1980s and 1990s (Lucht *et al.*, 2002). A full description can be found in Sitch *et al.* (2003). Processes governing water uptake by vegetation were updated by Gerten *et al.* (2004). In this study we used the version described in Sitch *et al.* (2003), including the changes implemented by Gerten *et al.* (2004), with an implementation of plant hydraulic architecture (for more details online see Appendix S1 in Supplementary Material) and further parameter updates. All the changes relative to the previously published model versions are described in detail online in Appendix S2 (see Supplementary Material).

The LPJ–DGVM accounts for the variety of structure and function among plants by representing vegetation as a mixture of plant functional types (PFTs; Table S1.2 in Appendix S1). These are distinguished based on bioclimatic limits (Sitch *et al.*, 2003), which determine the limits of the climatic space in which the PFT can potentially occur, and morphological, phenological and physiological and life-history characteristics, which influence growth and competition.

Physiological processes (e.g. photosynthesis, plant respiration and microbial decomposition) and associated fluxes of carbon and water between soil layers, vegetation and the atmosphere are simulated on a daily time step. Growth, litterfall, fine root turnover, vegetation dynamics and disturbance are simulated on an annual time step. Growth is calculated by allocating the annually accrued NPP to the biomass compartments leaves, sapwood and fine

© 2006 The Authors

roots according to a set of allometric rules, and a fixed fraction of sapwood is transformed into heartwood each year. Vegetation dynamics include the processes of establishment, mortality and disturbance by wildfires (Thonicke *et al.*, 2001).

Plant hydraulic architecture was accounted for within a new model formulation for calculating the supply of water to leaves. If the water supply is lower than the atmospheric demand, which is calculated based upon the leaf conductance associated with an optimum (no water shortage) photosynthesis rate, canopy conductance is reduced until plant transpiration equals the supply. Under these circumstances the diffusion of CO_2 into the leaf is also decreased, which results in lower photosynthesis rates, resulting in a dynamic feedback between fluxes of water and carbon (Ball *et al.*, 1987). Detailed model representations of assimilation and hydrology, the implementation of plant hydraulic architecture and the derivation of parameters for the hydraulic characteristics of roots, shoots and leaves of a global set of PFTs are given in Appendix S1.

Environmental input data

For simulations of global vegetation, global patterns of AET and runoff, as well as stand-scale NPP, the model was driven by gridded monthly data for air temperature, precipitation, number of rain days and sunshine hours from the global CRU05 data set (1901–2000; New *et al.*, 2000). Climate data for a 1000-year model spin-up were derived from the same data by repeating detrended values of the climate input for 1901–30, using preindustrial CO_2 content of the atmosphere. Monthly temperature and sunshine data were interpolated to provide 'quasi-daily' time series. Daily precipitation data were generated with a stochastic weather generator (Gerten *et al.*, 2004). Soil texture data were as in Sitch *et al.* (2003), based on the FAO soil data set (Zobler, 1986; FAO, 1991). A data set of historical global atmospheric CO_2 concentrations was obtained courtesy of the Carbon Cycle Model Linkage Project (McGuire *et al.*, 2001).

For the stand-scale simulations of AET, the model was driven with reconstructed climatic time series based on CRU05 and site climatology from the EUROFLUX project (Valentini, 2003; Morales *et al.*, 2005). Information on soil data and site history, which was implemented within the model for each stand, was also obtained from EUROFLUX. For young stands, site history was implemented by planting the forest in the same year and with the same stem density as reported from the site, and the model was run without natural mortality. Older stands were initiated in the same way, but the model was run with mortality, in order to account for natural mortality and forest thinning. Simulated values of leaf area index (LAI), standing biomass and stem density generally corresponded well to the observed forest structure during the period of the flux measurements.

Data for evaluation of model results

The global map of potential natural vegetation constructed by Haxeltine & Prentice (1996) was used to evaluate simulated patterns of vegetation distribution. The area designated 'temperate/boreal mixed forest' in southeastern United States was reclassified as 'temperate mixed forest' based on Küchler (1964). The simulated PFT composition was translated into vegetation classes for comparison purposes, using the classification rules given in Table 1, which were based on the vegetation type classification used by Haxeltine & Prentice (1996).

Modelled hydrological processes were tested against latitudinal estimates of average AET (Baumgartner & Reichel, 1975; Henning, 1989), stand-level eddy-covariance measurements of AET for various forest sites across Europe (EUROFLUX; P. Morales, pers. comm.) and latitudinal estimates of total runoff (Cogley, 1998).

NPP at a variety of sites covering different vegetation types was taken from the Ecosystem Model-Data Intercomparison (EMDI) database (Olson *et al.*, 2001). Only the sites with the highest data quality (class A) were used. These included 20 tropical forests, seven temperate forests, 23 boreal forests and 31 grasslands, distributed over all continents. All sites are 'seminatural', heavily managed sites and wetlands are not included in the data base (Olson *et al.*, 2001). Data on total NPP (above- and below-ground) was used for model-data intercomparison.

The map of potential vegetation, NPP data, as well as zonal-average estimates of AET and runoff, were compared to the average model predictions for 1961–90, which corresponds to the period in which most of the observational data has been collected. This period excludes the strong climate warming observed during the 1990s.

Comparison of vegetation maps

Agreement between the simulated pattern of global vegetation and potentially occurring vegetation was quantified using the kappa statistic (Prentice *et al.*, 1992). This statistic is derived by subtracting the agreement between two maps due to chance from the overall agreement. The result is normalized by the maximum possible value of difference (see Prentice *et al.*, 1992 for a detailed description). The kappa statistic is close to zero when agreement between two vegetation maps is no better than expected by chance, and reaches unity when agreement is perfect.

Kappa values were calculated for the entire globe, as well as for individual vegetation classes. The statistic can also be used to examine the agreement between two maps at scales larger than the grid size. Adjacent grid cells were grouped into blocks and the proportions of different classes within each block were calculated. The agreement between maps was then based on the similarity between the proportions of different classes found within the blocks.

RESULTS

Potential natural vegetation

In Fig. 1 simulated patterns of global vegetation are compared visually with potentially occurring vegetation. The overall value of the kappa statistic was 0.42, which indicates 'fair agreement' according to the classification scheme proposed by Monserud &

© 2006 The Authors

Table 1 Vegetation type classification scheme

Vegetation type	Tree LAI	Grass LAI[1]	Total LAI	Dominant tree PFT[2]
Boreal[3] deciduous forest/woodland	> 0.5			BNS
Boreal[3] evergreen forest/woodland	> 0.5			BNE or BBS
Temperate[4]/boreal mixed forest	> 2.5			
Temperate[3] conifer forest	> 2.5			TeNE
Temperate[3] deciduous forest	> 2.5			TeBS
Temperate[3] broadleaved evergreen forest	> 2.5			TeBE or TeSBE
Temperate mixed forest[3]	> 2.5			
Tropical seasonal forest[5]	> 2.5			
Tropical rain forest[6]	> 2.5			TrBE
Tropical deciduous forest[6]	> 2.5			TrBR
Moist savannas	< 2.5 and > 0.5		> 3	
Dry savannas	< 2.5 and > 0.5		≤ 3	
Tall grassland	< 0.5	> 3		
Dry grassland	< 0.2	> 0.5		
Xeric woodland/shrub	< 2.5 and > 0.5	< LAI_{trees}		
Arid shrubland/steppe	< 0.5		> 0.2	
Arctic/alpine tundra[7]	< 0.5		> 0.2	
Desert			< 0.2	

The plant functional types (PFTs) used in this table are boreal needle-leaved summergreen (BNS), boreal broadleaved summergreen (BBS), temperate needle-leaved evergreen (TeNE), temperate broadleaved summergreen (TeBS), temperate broadleaved evergreen (TeBE), temperate sclerophyllous broadleaved evergreen (TeSBE), tropical broadleaved evergreen (TeBE), and tropical broadleaved raingreen (TeBR). [1]Leaf area index (LAI) (maximum during the growing season). [2]Highest LAI among tree PFTs. [3]Boreal forest is mapped if $LAI_{boreal\ trees} > 0.8 \star$total tree LAI ($LAI_{trees}$); temperate forest if $LAI_{temperate\ trees} > 0.8 \star LAI_{trees}$. [4]Temperate/boreal mixed forest is mapped if $0.2 \star LAI_{trees} < LAI_{boreal\ trees} < 0.8 \star LAI_{trees}$ and $0.2 \star LAI_{trees} < LAI_{temperate\ trees} < 0.8 \star LAI_{trees}$. [5]Tropical seasonal forest is mapped if $LAI_{tropical\ trees} > 0.5 \star LAI_{trees}$, but neither LAI_{TrBE} nor $LAI_{TrBR} > 0.6 \star LAI_{trees}$. [6]Tropical rain forest is mapped if $LAI_{TrBE} > 0.6 \star LAI_{trees}$; tropical deciduous forest if $LAI_{TrBR} > 0.6 \star LAI_{trees}$. [7]Tundra is mapped if $LAI_{trees} < 0.5 \star LAI_{trees}$, and latitude > 54° N′ or the sum of growing degree days (GDD_5) < 350.

Leemans (1992). A higher level of agreement (kappa = 0.47) was achieved when the pixel size for comparison was increased to 2.5°, instead of comparing pixel by pixel (0.5° pixel size, i.e. original model resolution). Comparisons with the kappa statistic at spatial scales larger than the grid size are based on the proportions of different vegetation classes within each grid (Prentice *et al.*, 1992).

Kappa values for individual vegetation types are given in Table 2. The agreement between modelled and potentially occurring vegetation was generally highest for the major global forest types, arctic/alpine tundra and deserts. Exceptions were temperate conifer forests, which dominate only limited areas globally, and temperate broadleaved evergreen forests. However, in most areas where temperate broadleaved evergreen forests naturally dominate, i.e. in South-East Asia, southeastern Australia and New Zealand (Fig. 1b), the corresponding PFT [temperate broadleaved evergreen tree (TeBE)] was predicted to have the highest cover among all tree PFTs (results not shown), yet TeBE cover was below the 50% LAI threshold for the broadleaved evergreen vegetation type (Table 1).

The potential distribution of the different savanna and grassland vegetation classes was not accurately captured by the model (Fig. 1, Table 2). Generally, the model failed to predict the large savanna areas in South America and Africa, predicting forest vegetation instead.

Table 2 Kappa statistics for a global comparison of simulated vegetation patterns with potentially occurring natural vegetation

	Pixel size	
Vegetation type	0.5°	2.5°
Arctic/alpine tundra	0.74	0.80
Boreal deciduous forest/woodland	0.62	0.61
Boreal evergreen forest/woodland	0.63	0.65
Temperate/boreal mixed forest	0.43	0.46
Temperate conifer forest	0.10	0.20
Temperate deciduous forest	0.32	0.37
Temperate broadleaved evergreen forest	0.06	0.10
Temperate mixed forest	0.26	0.24
Tropical seasonal forest	0.41	0.45
Tropical rain forest	0.54	0.53
Tropical deciduous forest	0.25	0.32
Moist savanna	0.05	0.14
Dry savanna	0.08	0.12
Tall grassland	0.08	0.15
Short grassland	0.13	0.19
Xeric woodland/shrub	0.21	0.33
Arid shrubland/steppe	0.27	0.37
Desert	0.70	0.69

© 2006 The Authors

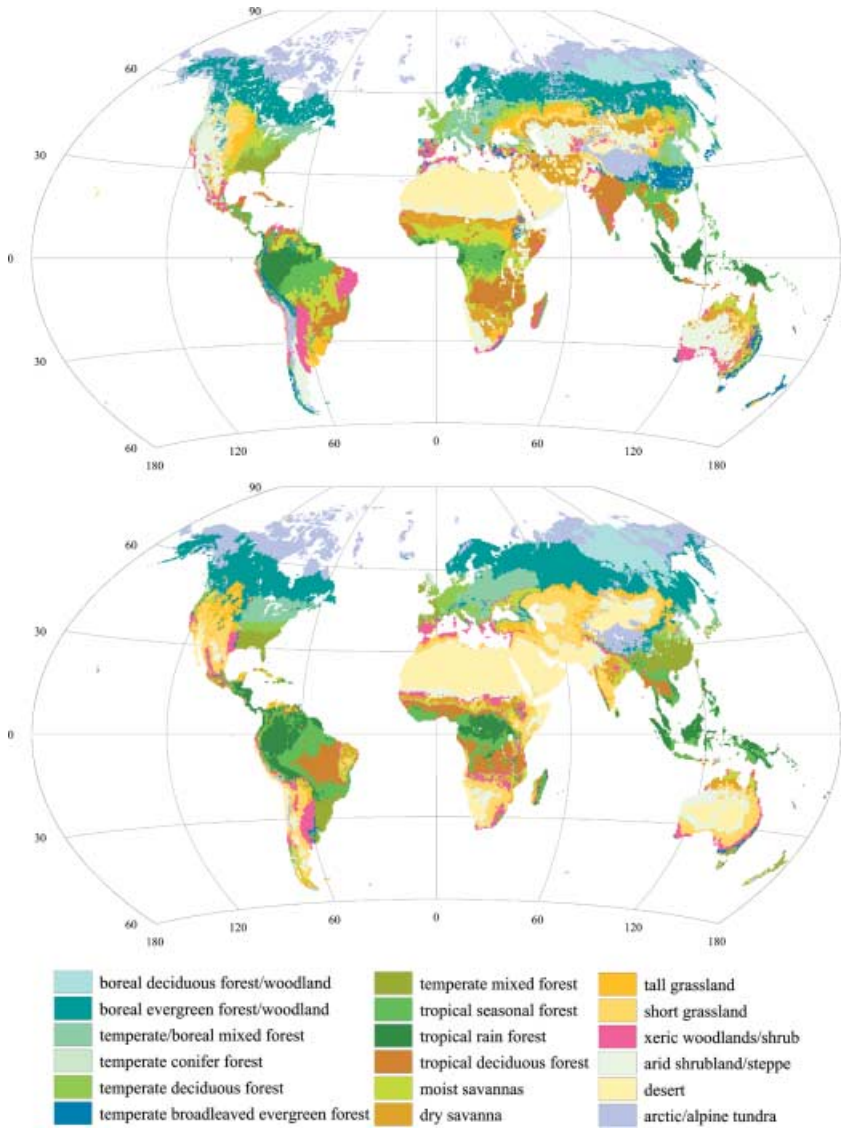

Figure 1 (a) Map of global potential natural vegetation (Haxeltine & Prentice, 1996; modified, see text). (b) Vegetation predicted by the model. The Winkel-Tripel (Canters & Declair, 1989) projection was used.

In order to assess the ability of the model to reproduce the general distribution of broadly defined vegetation types, the kappa statistic was also applied to a reduced set of vegetation classes, savannas and grasslands being treated as one vegetation class (Table 3). This comparison yielded a considerably higher kappa statistic (overall value 0.53) than the comparison with the full set of vegetation classes. The low overall kappa statistic value with the full set of vegetation classes was, thus, largely caused by the fact that the model failed to distinguish accurately between different grassland and savanna types.

Some additional discrepancies between modelled and potentially occurring vegetation occurred both with the full and the reduced set of vegetation classes. Even though the model captured the major extent of treeless vegetation in the temperate steppes of America and Asia, it failed to simulate the 'Prairie Peninsula' of the mid-continental United States, as well as the grasslands of eastern Argentina and Uruguay (Fig. 1). Furthermore, the model erroneously predicted grass or savanna vegetation in large parts of India where drought-deciduous forests naturally dominate, and the model predicted grasslands in some areas that are actually dominated by arid shrubland/steppe vegetation (most pronounced in the western United States).

Table 3 Kappa statistics for a global comparison of simulated vegetation patterns with potentially occurring natural vegetation with a reduced set of vegetation classes

	Pixel size	
Vegetation type	0.5°	2.5°
Forest/woodland	0.59	0.63
Grassland/savannas	0.31	0.36
Arid shrubland/steppe	0.27	0.37
Desert	0.70	0.69
Tundra	0.74	0.80

We also applied the model without plant hydraulic architecture (but otherwise identical input data and parameterization) using

© 2006 The Authors

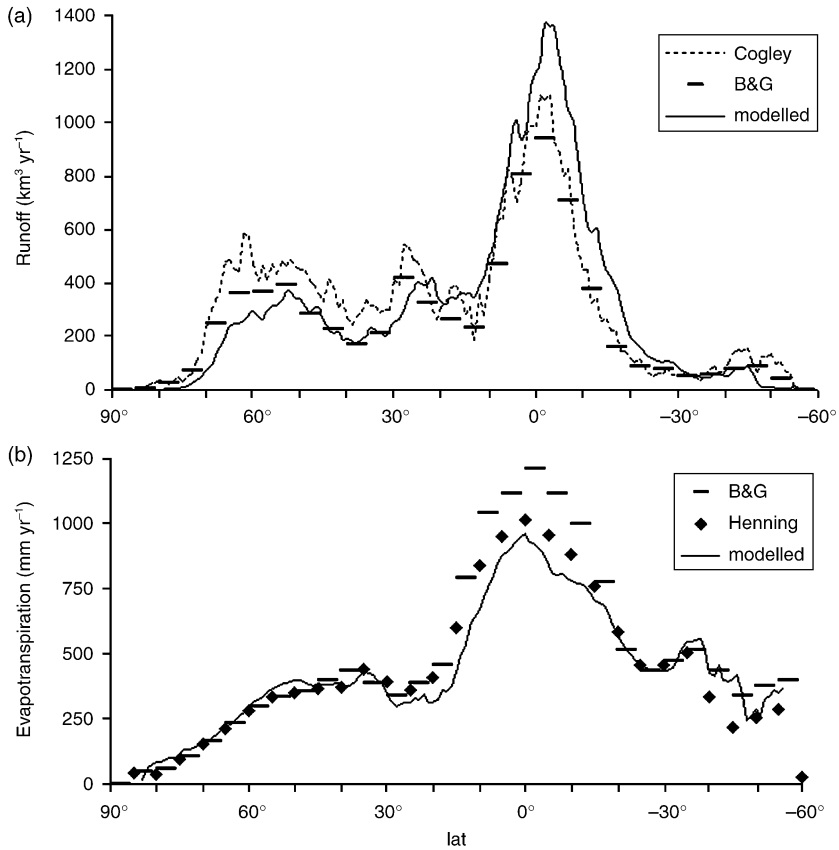

Figure 2 Estimates of long-term annual means of (a) total global runoff (km^3) and (b) average evapotranspiration (AET) from land (mm), aggregated into 1° or 5° latitudinal zones. The solid line represents the model simulations. The horizontal bars refer to estimates based on observed precipitation and runoff [Baumgartner & Reichel, 1975 (B&G in Figure)], and the broken line refers to observations from Cogley (1998). The diamonds in (b) represent AET calculated by Henning (1989).

the original, empirical model formulation for calculating the supply of water to plant leaves, which calculates plant-available water as a function of plant-root-weighted soil water content, soil texture and a maximum transpiration rate (Sitch *et al.*, 2003). When using the empirical formulation, the model achieved an overall kappa value of 0.40, which was slightly less than achieved with the implementation of plant hydraulic architecture (0.42). The formulation taking account of hydraulic architecture most strongly improved patterns of simulated vegetation in xeric woodland/shrub (Δkappa = 0.11) and arid shrubland/steppe (Δkappa = 0.06) vegetation.

Runoff and evapotranspiration

The model captured the broad global patterns of runoff and AET (Fig. 2a,b). Discrepancies between simulation results and data occurred in northern high latitudes, where the model underestimated runoff (Fig. 2a), and in the tropics, where the model overestimated runoff and underestimated AET (Fig. 2a,b).

The seasonal cycle of simulated AET corresponded well to observations from a variety of EUROFLUX sites (Fig. 3). The model failed to reproduce the observed seasonal cycle only at Collelongo, a Mediterranean site 1550 m above sea level (Fig. 3o), simulating a large reduction in AET during mid-summer, whereas the observed AET remained high throughout the growing season. The average error of the simulations expressed as the root mean square error scaled to the mean of the measurements (RMSE = 16.76 mm month^{-1}; Smith *et al.*, 1997) was within the range obtained with four other ecosystem models applied at the same EUROFLUX sites (Morales *et al.*, 2005). Averaged over all sites, the model overestimated AET by 6.42 mm month^{-1}. A test for significant over- or underestimation ($P < 0.05$) of the time-series data (Smith *et al.*, 1997; Morales *et al.*, 2005) revealed that the model overestimated AET at six sites, while AET was underestimated at one site. Overestimation of the observed AET was most pronounced for the two youngest forest plantations (Aberfeldy, Fig. 3a, stand age = 5 years in 1996, and Gunnarsholt, Fig. 3b, stand age = 3 years in 1996).

Comparison to NPP data

Linear correlation analysis identified one tropical C_4 grassland with exceptionally high productivity (799 g C m^{-2} year^{-1}) as an outlier, which was excluded from the analyses. The analysis with the reduced data set revealed a highly significant relationship between modelled and observed NPP values (Fig. 4; $R^2 = 0.36$; $P < 0.001$). However, the model generally predicted higher NPP values than in the observed data (Table 4): simulated NPP for forests was on average 18.8% higher, and simulated grassland NPP on average 50.2% higher than observed. The global total NPP was estimated by the model to be 45.5 Gt C year^{-1} (1 Gt = 1 billion tonnes). This estimate is at the lower end of the range of 44.4–66.3 Gt for terrestrial biogeochemistry models included in the Potsdam NPP Intercomparison project (Cramer *et al.*, 1999).

© 2006 The Authors

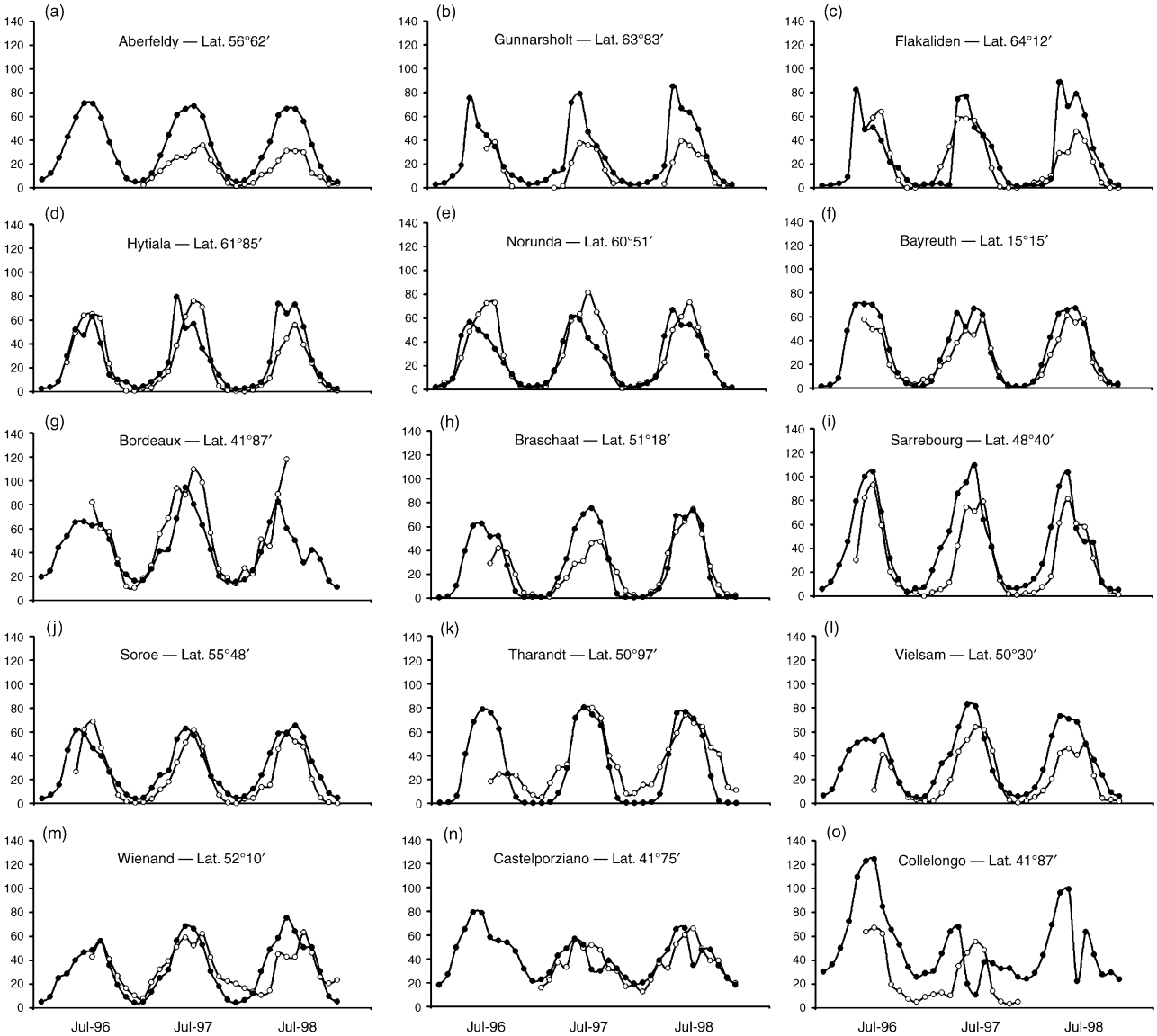

Figure 3 Measured (open symbols) and simulated (filled symbols) monthly AET (mm month^{-1}) for various European forest sites (EUROFLUX, 1996–98). Boreal conifers dominate at sites a, c, d, f, e, k and m. Site b is dominated by boreal broadleaved trees; site g by temperate conifers; sites j and o by temperate broadleaved trees; site n by Mediterranean evergreens. More information on site characteristics can be obtained from Morales *et al*. (2005).

DISCUSSION

Potential natural vegetation

The model generally reproduced observed patterns of global vegetation distribution in terms of broadly defined vegetation types, but it failed to distinguish accurately between different types of grassland and savanna vegetation. Possible explanations for major discrepancies between the model results and data are discussed below.

The low tree cover in the moist savannas of Venezuela (the Llanos) and several savanna areas of Africa, which the model predicted to be covered by forests, has been partly attributed to intensive laterization (Breckle, 2002), a feature not included in the model input data of soil characteristics. Laterite layers in the soil limit rooting depth; soils are often flooded for several months during the rainy season, while the soil layers accessible to plant roots dry out totally during the dry season. Grasses with ephemeral life histories are better adapted to this fluctuating environment than trees (Breckle, 2002). Low nutrient availability, particularly phosphorous, may also inhibit the growth of trees in African savannas (Scholes & Walker, 1993) and the savanna areas in central Brazil (Campos Cerrados; Breckle *et al*. 2002). In most areas where LPJ–DGVM overestimated forest cover, other vegetation models with similar environmental input data also tend to simulate higher forest cover (Prentice *et al*., 1992; Neilson & Marks, 1994; Haxeltine & Prentice, 1996; Friend & White, 2000; Kucharik *et al*., 2000; Cramer *et al*., 2001). In the cases of US 'Prairie Peninsula' and the grasslands in eastern Argentina (Pampas) the reasons for the low tree cover are less clear, but

© 2006 The Authors

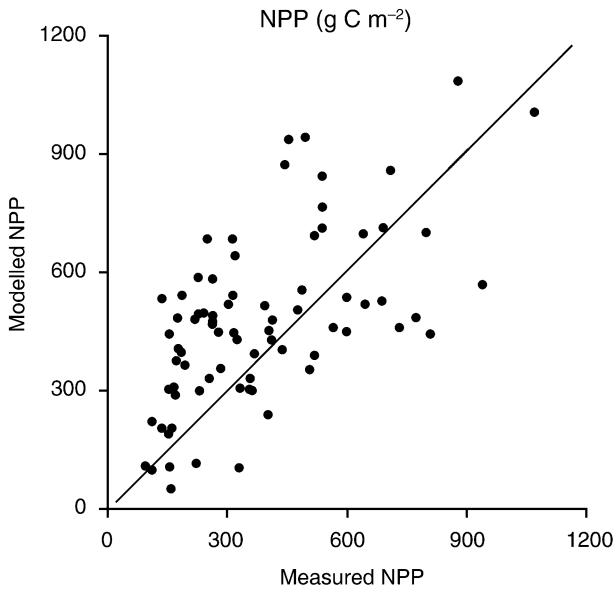

Figure 4 Modelled and measured NPP at study sites spanning multiple biomes from the EMDI data set. The solid line indicates exact agreement.

Table 4 Comparison between modelled annual NPP and NPP field measurements (EMDI data), averaged over all sites and for forests and grasslands sites separately. Standard deviations are given in parentheses

	All sites (g C m^{-2}) $N = 80$	Forests (g C m^{-2}) $N = 50$	Grasslands (g C m^{-2}) $N = 30$
Field data	377 (219)	469 (221)	223 (93)
Modelled	474 (214)	557 (195)	335 (163)

climate and soil texture, which were the only environmental model inputs in this study, may be insufficient as an explanation (Thompson *et al.*, 1999; Breckle, 2002).

In some areas, consideration of groundwater storage, which is not simulated in the LPJ–DGVM, may be necessary to accurately simulate the competitive balance between trees and grasses. Access to groundwater could be important for trees to compete successfully with grasses if precipitation is highly seasonal. The finely branched root systems of grasses are more efficient in extracting water from upper soil layers, while trees may access water stored deep in the soil and thereby remain active through the dry season (Breckle, 2002; Pärtel & Wilsona, 2002). The absence of this mechanism may, for example, explain why the model underestimated forest cover in monsoonal areas of India, where rainfall is plentiful but highly seasonal. A further possibility is that the generalized fire module may not be sophisticated enough to adequately model the effects of fire, which occurs regularly in most savanna environments, on the competitive balance between trees and grasses.

The improvement of simulated vegetation patterns in xeric and arid vegetation types, compared to the original version of the model with its empirical formulation for calculating water availability, suggests that the inclusion of differences in plant hydraulic architecture is particularly important when simulating vegetation changes in these areas. Sclerophyllous plants with special hydraulic characteristics (see Appendix S1 in Supplementary Material) often play an important role in these dry ecosystems.

Runoff and evapotranspiration

The model underestimated runoff in high northern latitudes (Fig. 2a), possibly because permafrost was not considered in this study. Permafrost limits the depth to which water can be stored in the soil, which increases runoff. Preliminary simulations of an active permafrost layer in the LPJ–DGVM substantially improved runoff estimates for subarctic regions (C. Beer, unpublished data).

It is possible that the water balance of some tropical regions was not accurately captured by the LPJ–DGVM (Fig. 2b) because the model currently does not explicitly distinguish wetlands, which cover large areas in the tropics and generate considerable evaporation (Melillo *et al.*, 1993).

With the exception of two young forest plantations, simulated AET was in the same general range as observed at the EUROFLUX forests (Fig. 3), with a tendency to slightly overestimate the magnitude of AET. The large discrepancy for the two young plantations, where canopy closure has not yet been reached, suggests that the model overestimated evaporation from the ground surface. The overall tendency to simulate higher AET than observed could have the same explanation, but other possible causes include an overestimation of the atmospheric water vapour demand or an underestimation of the hydraulic resistances along the root–plant–atmosphere pathway. Peak-growing season AET at the Mediterranean sites (in particular at Collelongo) was probably underestimated by the model because tree access to groundwater storage was not considered.

Comparison to NPP data

In spite of uncertainty associated with potential scaling mismatches when comparing grid-based model output with stand-scale field measurements of NPP (Zheng *et al.*, 2003), as well as considerable uncertainty in NPP field measurements (e.g. Chapin *et al.*, 2002), modelled NPP values showed strong overall correlation with observations. However, the model tended to simulate higher NPP than given in the EMDI data set, in particular for grasslands. Two factors may primarily explain this discrepancy between model results and data.

First, NPP in grasslands is generally limited by water availability and, under dry conditions, the hydraulic resistance to water flow in the soil may limit water uptake and thereby NPP (Sperry *et al.*, 1998; Williams *et al.*, 1998; Sperry & Hacke, 2002). In this study, the hydraulic resistance of the soil–root pathway was neglected because it is difficult to measure directly, and theoretical models depend on assumptions concerning detailed soil characteristics, as well as rooting density and root structure (Newman, 1969; Sperry *et al.*, 1998). Such data are not available for large areas or as gridded data sets.

© 2006 The Authors

In the case of grasslands, another explanation may be that the NPP values given in the EMDI data set underestimate the true NPP. Grassland productivity has commonly been estimated using annual maximum standing biomass (House & Hall, 2001; Scurlock *et al*., 2002). This method does not, for example, account for below-ground productivity, the effects of grazing and trampling and mortality before or growth after the attainment of peak standing biomass (House & Hall, 2001). Some estimates of grassland production are 2–5 times higher when these factors are accounted for (Long *et al*., 1989; Scurlock *et al*., 2002). Too-low productivity values in the data set could also explain why, in spite of the overestimation of NPP compared with EDMI data, the total global NPP simulated by the model was at the lower end of the range predicted by other biogechemistry models (Cramer *et al*., 1999).

CONCLUSIONS

In this study, we show that a version of the LPJ–DGVM that includes a new mechanistic treatment of water flow through plants reproduces observed patterns of global vegetation distribution, terrestrial ecosystem water cycling and variations of NPP across biomes. The presented model makes it possible to mechanistically resolve the effects of hydraulic differences between PFTs on vegetation structure, water cycling and competition.

Including aspects of hydraulic architecture within process-based vegetation models also increases the functional diversity of the combination of PFTs making up the vegetation. As functional diversity is considered to be a fundamental factor affecting the stability of ecosystems and their resilience to perturbation (Tilman *et al*., 1997; Loreau *et al*., 2001), this may be an advantage when modelling future ecosystem responses to climate change.

During recent years, plant hydraulic architecture has received increasing attention within ecological research. Results of this research may lead to a better understanding of the processes controlling hydraulic fluxes, leading to improved parameter estimates for usage in large-scale models that include the relevant processes. The presented modelling framework can be used to implement alternative hypotheses and parameter values concerning the effects of hydraulic architecture, which can then be tested against data on vegetation distribution and ecosystem processes at scales from the stand to the biosphere.

ACKNOWLEDGEMENTS

We thank Dieter Gerten for providing data on global runoff (Baumgartner & Reichel, 1975; Cogley, 1998) and AET (Baumgartner & Reichel, 1975; Henning, 1989). The EUROFLUX research community (especially Timo Vesala, Paul Berbigier, Oliver Bouriaud, Wilma Jans, Giorgio Mateucci and Marc Aubinet) and Pablo Morales are acknowledged for providing monthly AET values, interpolated climate data and information on site history from the EUROFLUX project. The CRU05 climate data were supplied courtesy of the Climatic Research Unit, University of East Anglia. Thomas Hickler was partly funded from the two EU FP6 projects ALARM (contract number GOCE-CT-2003-506675) and ENSEMBLES (contract number GOCE-CT-2003-505539).

REFERENCES

Ball, J.T., Woodrow, I.E. & Berry, J.A. (1987) A model predicting stomatal conductance and its contribution to the control of photosynthesis under different environmental conditions. *Progress in Photosynthesis Research*, **4**, 221–224.

Baumgartner, A. & Reichel, E. (1975) *Die Weltwasserbilanz*. R. Oldenburg Verlag, Munich.

Bond, B.J. & Kavanagh, K. (1999) Stomatal behaviour of four woody species in relation to leaf-specific hydraulic conductance and threshold water potential. *Tree Physiology*, **19**, 503–510.

Breckle, S.W. (2002) *Walter's vegetation of the earth: the ecological systems of the geo-biosphere*. Springer, Berlin.

Canters, F. & Declair, H. (1989) *The world in perspective — a directory of world map projections*. John Wiley & Sons Ltd, Chichester, U.K.

Chapin, F.S. III, Matson, P.A. & Mooney, H.A. (2002) *Principles of terrestrial ecosystem ecology*. Springer, New York.

Cogley, J.G. (1998) *GGHYDRO — global hydrographic data, release 2.2. Data set*. Available online [http://www.trentu.ca/geography/glglgghy.htm] from Department of Geography. Trent University, Peterborough, Ontario, Canada.

Costanza, R., d'Arge, R., de Groot, R., Farber, S., Grasso, M., Hannon, B., Limburg, K., Naeem, S., O'Neill, R.V., Paruelo, J., Raskin, R.G., Sutton, P. & van den Belt, M. (1997) The value of the world's ecosystem services and natural capital. *Nature*, **387**, 253–260.

Cramer, W., Bondeau, A., Woodward, F.I., Prentice, I.C., Betts, R.E., Brovkin, V., Cox, P.M., Fisher, V., Foley, J.A., Friend, A.D., Kucharik, C., Lomas, M.R., Ramankutty, N., Sitch, S., Smith, B., White, A. & Young-Molling, C. (2001) Global response of terrestrial ecosystem structure and function to CO_2 and climate change: results from six dynamic global vegetation models. *Global Change Biology*, **7**, 357–373.

Cramer, W., Kicklighter, D.W., Bondeau A., Moore, B. III, Churkina, G., Nemry, B., Ruimy, A., Schloss, A.L. & the participants of the Potsdam NPP model intercomparison (1999) Comparing global models of terrestrial net primary productivity (NPP): overview and key results. *Global Change Biology*, **5**, 1–16.

Farquhar, G.D., von Caemmerer, S. & Berry, J.A. (1980) A biochemical model of photosynthetic CO_2 assimilation in leaves of C_3 plants. *Planta*, **149**, 78–90.

Foley, J.A., Kutzbach, J.E., Coe, M.T. & Levis, S. (1994) Feedbacks between climate and boreal forests during the Holocene epoch. *Nature*, **371**, 52–54.

Foley, J.A., Prentice, I.C., Ramankutty, N., Levis, S., Pollard, D., Sitch, S. & Haxeltine, A. (1996) An integrated biosphere model of land surface processes, terrestrial carbon balance, and vegetation dynamics. *Global Biogeochemical Cycles*, **10**, 603–628.

Food and Agriculture Organization (FAO) (1991) *The digitized soil map of the world (release 1.0)*. FAO, Rome.

Friend, A.D. & White, A. (2000) Evaluation and analysis of a dynamic terrestrial ecosystem model under preindustrial conditions at the global scale. *Global Biochemical Cycles*, **14**, 1173–1190.

© 2006 The Authors

Gerten, D., Schabhoff, S., Haberlandt, U., Lucht, W. & Sitch, S. (2004) Terrestrial vegetation and water balance — hydrological evaluation of a dynamic global vegetation model. *Journal of Hydrology*, **286**, 249–270.

Haxeltine, A. & Prentice, I.C. (1996) BIOME3: an equilibrium terrestrial biosphere model based on ecophysiological constraints, resource availability, and competition among plant functional types. *Global Biochemical Cycles*, **10**, 693–709.

Henning, D. (1989) *Atlas of the surface heat balance of the continents.* Gebrüder Bornträger, Berlin, Stuttgart.

Houghton, J.T., Ding, Y., Griggs, D.J., Noguer, M., van der Linden, P.J., Dai, X., Maskell, K. & Johnson, C.A. (eds) (2001) *Climate change 2001: the scientific basis. Contribution of the working group I to the third assessment report of the International Panel of Climate Change.* Cambridge University Press, New York.

House, J.I. & Hall, D.O. (2001) Productivity of tropical savannas and grasslands. *Terrestrial global productivity* (ed. by J. Roy, B. Saugier and H.A. Mooney), pp. 363–400. Academic Press, San Diego.

Joos, F., Prentice, I.C., Sitch, S., Meyer, R., Hooss, G., Plattner, G.K., Gerber, S. & Hasselmann, K. (2001) Global warming feedbacks on terrestrial carbon uptake under the Intergovernmental Panel on Climate Change (IPCC) emission scenarios. *Global Biochemical Cycles*, **15**, 891–907.

Kucharik, C.J., Foley, J.A., Delire, C., Fisher, V.A., Coe, M.T., Lenters, J.D., Young-Molling, C., Ramankutty, N., Norman, J.M. & Gower, S.T. (2000) Testing the performance of a Dynamic Global Ecosystem Model: water balance, carbon balance, and vegetation structure. *Global Biogeochemical Cycles*, **14**, 795–825.

Küchler, A.W. (1964) *Potential natural vegetation of the conterminous United States.* American Geographical Society, New York.

Long, S.P., Garcia Moya, E., Imbamba, S.K., Kamnalrut, A., Piedade, M.T.F., Scurlock, J.M.O., Shen, Y.K. & Hall, D.O. (1989) Primary productivity of natural grass ecosystems of the tropics: a reappraisal. *Plant and Soil*, **115**, 155–166.

Loreau, M., Naeem, S., Inchausti, P., Bengtsson, J., Grime, J.P., Hector, A., Hooper, D.U., Huston, M.A., Raffaelli, D., Schmid, B., Tilman, D. & Wardle, D.A. (2001) Biodiversity and ecosystem functioning: current knowledge and future challenges. *Science*, **294**, 804–808.

Luan, J.S., Muetzelfeldt, R.I. & Grace, J. (1996) Hierarchical approach to forest ecosystem simulation. *Ecological Modelling*, **86**, 37–50.

Lucht, W., Prentice, I.C., Myneni, R.B., Sitch, S., Friedlingstein, P., Cramer, W., Bousquet, P., Buermann, W. & Smith, B. (2002) Climatic control of the high-latitude vegetation greening trend and Pinatubo effect. *Science*, **296**, 1687–1689.

Magnani, F., Mencuccini, M. & Grace, J. (2000) Age-related decline in stand productivity: the role of structural acclimation under hydraulic constraints. *Plant, Cell and Environment*, **23**, 251–263.

Mäkelä, A. (2003) Process-based modelling of tree and stand growth: towards a hierarchical treatment of multiscale processes. *Canadian Journal of Forest Research*, **33**, 398–409.

McDowell, N., Barnard, H., Bond, B., Hinckley, T., Hubbard, R., Ishii, H., Köstner, B., Magnani, F., Marshall, J., Meinzer, F., Phillips, N., Ryan, M. & Whitehead, D. (2002) The relationship between tree height and leaf area: sapwood area ratio. *Oecologia*, **132**, 12–20.

McGuire, A.D., Sitch, S., Clein, J.S., Dargaville, R., Esser, G., Foley, J., Heimann, M., Joos, F., Kaplan, J., Kicklighter, D.W., Meier, R.A., Melillo, J.M., Moore, B., Prentice, I.C., Ramankutty, N., Reichenaum, T., Schloss, A., Tian, H., Williams, L.J. & Wittenberg, U. (2001) Carbon balance of the terrestrial biosphere in the twentieth century: analyses of CO_2, climate and land use effects with four process-based ecosystem models. *Global Biogeochemical Cycles*, **15**, 183–206.

Melillo, J.M., McGuire, A.D., Kicklighter, D.W., Moore, B., Vorosmarty, C.J. & Schloss, A.L. (1993) Global climate change and terrestrial net primary production. *Nature*, **363**, 234–240.

Mencuccini, M. & Grace, J. (1996) Hydraulic conductance, light interception and needle nutrient concentration in Scots pine stands and their relations with net primary productivity. *Tree Physiology*, **16**, 459–468.

Monserud, R.A. & Leemans, R. (1992) Comparing global vegetation maps with the Kappa statistic. *Ecological Modelling*, **62**, 275–293.

Moorcroft, P.R., Hurtt, G.C. & Pacala, S.W. (2001) A method for scaling vegetation dynamics: the ecosystem demography model (ED). *Ecological Monographs*, **71**, 557–586.

Morales, P., Sykes, M.T., Prentice, I.C., Smith, P., Smith, B., Bugmann, H., Zierl, B., Friedlingstein, P., Viovy, N., Sabaté, S., Sánchez, A., Pla, E., Gracia, C.A., Sitch, S., Arneth, A. & Ogee, J. (2005) Comparing and evaluating process-based ecosystem model predictions of carbon and water fluxes in major European forest biomes. *Global Change Biology*, **11**, 1–13.

Neilson, R.P. (1995) A model for predicting continental scale vegetation distribution and water balance. *Ecological Applications*, **5**, 362–385.

Neilson, R.P. & Marks, D. (1994) A global perspective of regional vegetation and hydrologic sensitivities from climate change. *Journal of Vegetation Science*, **5**, 715–730.

New, M., Hulme, M. & Jones, P. (2000) Representing twentieth-century space-time climate variability. Part II. Development of 1901–96 monthly grids of terrestrial surface climate. *Journal of Climate*, **13**, 2217–2238.

Newman, E.I. (1969) Resistance to water flow in soil and plant. I. Soil resistance in relation to amounts of root: theoretical estimates. *Journal of Applied Ecology*, **6**, 1–12.

Olson, R.J., Scurlock, J.M.O., Prince, S.D., Zheng, D.L. & Johnson, K.R. (2001) NPP multi-biome: NPP and driver data for ecosystem model-data intercomparison. Data set. Available on-line [http://www.daac.ornl.gov] from the Oak Ridge National Laboratory Distributed Active Archive Center, Oak Ridge, Tennessee, USA.

Pärtel, M. & Wilsona, S.D. (2002) Root dynamics and spatial patterns in prairie and forest. *Ecology*, **83**, 1199–1203.

Prentice, I.C., Cramer, W., Harrison, S., Leemans, R., Monserud, R.A. & Solomon, A.M. (1992) A global biome model based on plant physiology and dominance, soil properties and climate. *Journal of Biogeography*, **19**, 117–134.

Prentice, I.C., Farquhar, G.D., Fasham, M.J.R., Goulden, M.L., Heimann, M., Jaramillo, V.J., Kheshgi, H.S., Le Quere, C., Scholes, R.J. & Wallace, D.W.R. (2001) The carbon cycle and

© 2006 The Authors

atmospheric carbon dioxide. *Climate change 2001: the scientific basis. Contribution of the working group I to the third assessment report of the international panel of climate change* (ed. by J.T. Houghton, Y. Ding, D.J. Griggs, M. Noguer, P.J. van der Linden, X. Dai, K. Maskell & C.A. Johnson), pp. 183–239. Cambridge, Cambridge University Press.

Ryan, M.G. & Yoder, B.J. (1997) Hydraulic limits to tree height and tree growth. *Bioscience*, **47**, 235–242.

Schäfer, K.V.R., Oren, R. & Tenhunen, J.D. (2000) The effect of tree height on crown level stomatal conductance. *Plant, Cell and Environment*, **23**, 365–375.

Schimel, D., Melillo, J., Tian, H., McGuire, A.D., Kicklighter, D., Kittel, T., Rosenbloom, N., Running, S., Thornton, P., Ojima, D., Parton, W., Kelly, R., Sykes, M., Neilson, R. & Rizzo, B. (2000) Contribution of increasing CO_2 and climate to carbon storage by ecosystems in the United States. *Science*, **287**, 2004–2005.

Scholes, R.J. & Walker, B.H. (1993) *An African savanna: synthesis of the Nylsvley study*. Cambridge University Press, Cambridge.

Scurlock, J.M.O., Johnson, K. & Olson, R.J. (2002) Estimating net primary productivity from grassland biomass dynamics measurements. *Global Change Biology*, **8**, 736–753.

Sitch, S., Brovkin, V., von Bloh, W., van Vuuren, D., Eickhout, B. & Ganopolski, A. (2005) Impacts of future land cover changes on atmospheric CO_2 and climate. *Global Biochemical Cycles*, **19**, GB2013.

Sitch, S., Smith, B., Prentice, I.C., Arneth, A., Bondeau, A., Cramer, W., Kaplan, J., Levis, S., Lucht, W., Sykes, M., Thonicke, K. & Venevsky, S. (2003) Evaluation of ecosystem dynamics, plant geography and terrestrial carbon cycling in the LPJ Dynamic Global Vegetation Model. *Global Change Biology*, **9**, 161–185.

Smith, B., Prentice, I.C. & Sykes, M.T. (2001) Representation of vegetation dynamics in the modelling of terrestrial ecosystems: comparing two contrasting approaches within European climate space. *Global Ecology and Biogeography*, **10**, 621–637.

Smith, P., Smith, J.U., Powlson, D.S., McGill, W.B., Arah, J.R.M., Chertov, O.G., Coleman, K., Franko, U., Frolking, S., Jenkinson, D.S., Jensen, L.S., Kelly, R.H., Klein-Gunnewiek, H., Komarov, A., Li, C., Molina, J.A.E., Mueller, T., Parton, W.J., Thornley, J.H.M. & Whitmore, A.P. (1997) A comparison of the performance of nine soil organic matter models using seven long-term experimental datasets. *Geoderma*, **81**, 153–225.

Sperry, J.S. & Hacke, U.G. (2002) Desert shrub water relations with respect to soil characteristics and plant functional type. *Functional Ecology*, **16**, 367–378.

Sperry, J.S., Adler, F.R., Campbell, B.D. & Comstock, J.P. (1998) Limitation of plant water use by rhizosphere and xylem conductance: results from a model. *Plant, Cell and Environment*, **21**, 347–359.

Sperry, J.S., Hacke, U.G., Oren, R. & Comstock, J.P. (2002) Water deficits and hydraulic limits to leaf water supply. *Plant, Cell and Environment*, **25**, 251–263.

Thompson, R.S., Anderson, K.H. & Bartlein, P.J. (1999) *Atlas of relations between climatic parameters and distributions of important trees and shrubs in North America. A: introduction and conifers.* US Geological Survey, Washington DC.

Thonicke, K., Vevevsky, S., Sitch, S. & Cramer, W. (2001) The role of fire disturbance for global vegetation dynamics: coupling fire into a dynamic global vegetation model. *Global Ecology and Biogeography*, **6**, 483–495.

Tilman, D., Knops, J., Wedin, D., Reich, P., Ritchie, M. & Siemann, E. (1997) The influence of functional diversity and composition on ecosystem processes. *Science*, **277**, 1300–1302.

Tyree, M.T. (2003) Hydraulic limits on tree performance: transpiration, carbon gain and growth of trees. *Trees*, **17**, 95–100.

Valentini, R. (ed.) (2003) *Carbon, water and energy exchanges of European forests*. Springer, Heidelberg.

VEMAP Members (1995) Vegetation/ecosystem modelling and analysis project: comparing biogeography and biogeochemistry models in a continental-scale study of terrestrial ecosystem responses to climate change and CO_2 doubling. *Global Biochemical Cycles*, **9**, 407–437.

Whitehead, D. (1998) Regulation of stomatal conductance and transpiration in forest canopies. *Tree Physiology*, **18**, 633–644.

Williams, M., Malhi, Y., Nobre, A.D., Rastetter, E.B., Grace, J. & Pereira, M.G.P. (1998) Seasonal variation in net carbon exchange and evapotranspiration in a Brazilian rain forest: a modelling analysis. *Plant, Cell and Environment*, **21**, 953–968.

Woodward, F.I., Smith, T.M. & Emanuel, W.R. (1995) A global land primary productivity and phytogeography model. *Global Biochemical Cycles*, **9**, 471–490.

Zheng, D.L., Prince, S. & Wright, R. (2003) Terrestrial net primary production estimates for 0.5° grid cells from field observations — a contribution to global biogeochemical modeling. *Global Change Biology*, **9**, 46–64.

Zimmermann, M.H. (1978) Hydraulic architecture of some diffuse-porous trees. *Canadian Journal of Botany*, **56**, 2286–2295.

Zobler, L. (1986) A world soil file for global climate modelling. *NASA Technical Memorandum*, **87802**, 32.

BIOSKETCH

Thomas Hickler is a postdoctoral fellow at the Department of Physical Geography and Ecosystems Analysis of Lund University. His main research interest is the development of mechanistic models of ecosystem structure and functioning, in particular under consideration of processes acting on different levels of ecological hierarchy.

Editor: David Currie

SUPPLEMENTARY MATERIAL

The following material is available from www.blackwell-synergy.com/loi/geb

Appendix S1 Detailed model representations of assimilation and hydrology, and the implementation of plant hydraulic architecture

Appendix S2 Updates of model parameter values

© 2006 The Authors